

MULTI-CHANNEL ALGEBRAIC SCATTERING THEORY AND THE STRUCTURE OF EXOTIC COMPOUND NUCLEI

K. AMOS* and P. FRASER*

*School of Physics, Melbourne University,
Victoria 3010, Australia*

*E-mail: amos@physics.unimelb.edu.au; pfraser@physics.unimelb.edu.au

D. van der KNIJFF*

*Advanced Computing Research, Information Division,
Melbourne University, Victoria 3010, Australia*

*E-mail: dirk@unimelb.edu.au

L. Canton* and G. Pisent*

*Istituto Nazionale di Fisica Nucleare, sezione di Padova,
e Dipartimento di Fisica dell'Università di Padova,
via Marzolo 8, Padova I-35131*

*E-mail: luciano.canton@pd.infn.it; gualtiero.pisent@pd.infn.it

S. Karataglidis*

*Department of Physics and Electronics, Rhodes University,
Grahamstown 6140, South Africa*

*E-mail: S.Karataglidis@ru.ac.za

J. P. Svenne*

*Department of Physics and Astronomy, University of Manitoba,
and Winnipeg Institute for Theoretical Physics,
Winnipeg, Manitoba, Canada R3T 2N2*

*E-mail: svenne@physics.umanitoba.ca

A Multi-Channel Algebraic Scattering (MCAS) theory is presented with which the properties of a compound nucleus are found from a coupled-channel problem. The method defines both the bound states and resonances of the compound nucleus, even if the compound nucleus is particle unstable. All resonances of the system are found no matter how weak and/or narrow. Spectra of mass-7 nuclei and of ^{15}F , and MCAS results for a radiative capture cross section are presented.

Keywords: Coupled-channel theory, compound-nucleus spectra, capture cross sections

1. Introduction

The MCAS method^{1,2} has been formed to solve coupled-channel Lippmann-Schwinger equations for a chosen two-body system. The theory is built upon sturmian expansions of whatever one chooses to be the matrix of interaction potential functions for the system. The set of sturmians that form the basis of the expansions are determined from the self-same interaction potentials and, if necessary, can be selected to ensure that the Pauli principle is not violated. The approach, which is most suited to deal with low energies, facilitates a systematic determination of all sub-threshold bound and resonance states of the compound nucleus within any energy range considered.

While the required starting matrix of potentials may be constructed from any model of nuclear structure, to date we have used just a simple collective rotational model to define those potentials with deformation taken to second order. Also, to date only low energy scattering from light mass nuclei have been considered so that just the ground, first, and second excited states of the target nucleus have been used to define the channel couplings.

Isospin symmetry in mirror scattering systems, save only for inclusion of the Coulomb interaction, has been used with MCAS to estimate the spectra of nuclei that are just outside of the proton drip line. ¹⁵F is one such case.³ The $A = 7$ system also has been considered and, with a unique nuclear potential, the level structures of ⁷He, ⁷Li, ⁷Be, and ⁷B have been obtained.² We have also used the scheme to consider low energy properties of ³H-⁴He and ³He-⁴He scattering to correlate different views of the spectra of ⁷Li and ⁷Be. Using the di-cluster structure of ⁷Be found using MCAS, the astrophysical S -factor for the radiative capture of ³He by ⁴He has been evaluated.

2. The MCAS theory

In brief, the MCAS approach is based upon using sturmian functions as a basis set to expand the chosen interaction potentials. Each element in the interaction matrix then is a sum of separable interactions. The analytic properties of the S -matrix from a separable Schrödinger potential gives the means by which a full algebraic solution of the multichannel scattering problem can be realized. As all details of the MCAS theory have been published,¹ only salient features are repeated herein. Consider a coupled-channel system for each allowed scattering spin-parity J^π . With the MCAS method, one solves the Lippmann-Schwinger (LS) integral equations in momentum space, i.e.

$$T_{cc'}(p, q; E) = V_{cc'}(p, q) + \frac{2\mu}{\hbar^2} \left[\sum_{c''=1}^{\text{open}} \int_0^\infty V_{cc''}(p, x) \frac{x^2}{k_{c''}^2 - x^2 + i\epsilon} T_{c''c'}(x, q; E) dx - \sum_{c''=1}^{\text{closed}} \int_0^\infty V_{cc''}(p, x) \frac{x^2}{\hbar^2 + x^2} T_{c''c'}(x, q; E) dx \right], (1)$$

where the index c denotes the quantum numbers that identify each channel uniquely. Such requires specification of potential matrices $V_{cc'}^{(J^\pi)}(p, q)$. The open and closed channels have channel wave numbers k_c and h_c for $E > \epsilon_c$ and $E < \epsilon_c$ respectively, and μ is the reduced mass. Solutions of Eq. (1) are sought using expansions of the potential matrix elements in (finite) sums of energy-independent separable terms,

$$V_{cc'}(p, q) \sim \sum_{n=1}^N \chi_{cn}(p) \eta_n^{-1} \chi_{c'n}(q). \quad (2)$$

The key to the method is the choice of the expansion form factors $\chi_{cn}(q)$. Optimal ones have been found from the sturmian functions that are determined from the actual (coordinate space) model interaction $V_{cc'}(r)$ initially chosen to describe the coupled-channel problem. The η_n are energy scales associated with the sturmian functions. Details are given elsewhere.¹

Calculations of the multichannel T - and scattering (S -) matrices involve a Green's function matrix,

$$(G_0)_{nn'} = \frac{2\mu}{\hbar^2} \left[\sum_{c=1}^{\text{open}} \int_0^\infty \chi_{cn}(x) \frac{x^2}{k_c^2 - x^2 + i\epsilon} \chi_{c'n'}(x) dx - \sum_{c=1}^{\text{closed}} \int_0^\infty \chi_{cn}(x) \frac{x^2}{h_c^2 + x^2} \chi_{c'n'}(x) dx \right], \quad (3)$$

The bound states of the compound system are defined by the zeros of matrix determinant for energy $E < 0$, namely the zeros of $\{[\boldsymbol{\eta} - \mathbf{G}_0]\}$ when all channels in Eq. (3) are closed. The $\boldsymbol{\eta}$ is a diagonal matrix with entries $(\eta)_{nn'} = \eta_n \delta_{nn'}$.

Elastic scattering observables are determined by the on-shell values ($k_1 = k_1' = k$) of the scattering matrices. For the elastic scattering of neutrons (spin $\frac{1}{2}$) from spin-zero targets $c = c' = 1$, and $S_{11} \equiv S_\ell^J = S_\ell^{(\pm)}$ are,¹

$$S_{11} = 1 - i\pi \frac{2\mu k}{\hbar^2} \sum_{nn'=1}^M \chi_{1n}(k) \frac{1}{\sqrt{\eta_n}} \left[\left(\mathbf{1} - \boldsymbol{\eta}^{-\frac{1}{2}} \mathbf{G}_0 \boldsymbol{\eta}^{-\frac{1}{2}} \right)^{-1} \right]_{nn'} \frac{1}{\sqrt{\eta_{n'}}} \chi_{1n'}(k). \quad (4)$$

Diagonalization of the complex-symmetric matrix,

$$\sum_{n'=1}^N \eta_n^{-\frac{1}{2}} [\mathbf{G}_0]_{nn'} \eta_{n'}^{-\frac{1}{2}} \tilde{Q}_{n'r} = \zeta_r \tilde{Q}_{nr}, \quad (5)$$

establishes the evolution of the complex eigenvalues ζ_r with respect to energy. Resonant behavior occurs when an eigenvalue, ζ_r , as a function of E , crosses the unit circle in the Gauss plane near the point (1,0). It is evident that the elastic channel S matrix has a pole structure at the corresponding energy where the modulus of one of these eigenvalues approach unity, since

$$\left[\left(\mathbf{1} - \boldsymbol{\eta}^{-\frac{1}{2}} \mathbf{G}_0 \boldsymbol{\eta}^{-\frac{1}{2}} \right)^{-1} \right]_{nn'} = \sum_{r=1}^N \tilde{Q}_{nr} \frac{1}{1 - \zeta_r} \tilde{Q}_{n'r}. \quad (6)$$

3. Results

3.1. The spectrum of ^{15}F ($p+^{14}\text{O}$)

Spectra, known and calculated (using MCAS³) for ^{15}C and ^{15}F , are shown in Fig. 1. The known properties of ^{15}C agree well with MCAS results for the $n+^{14}\text{C}$ system.

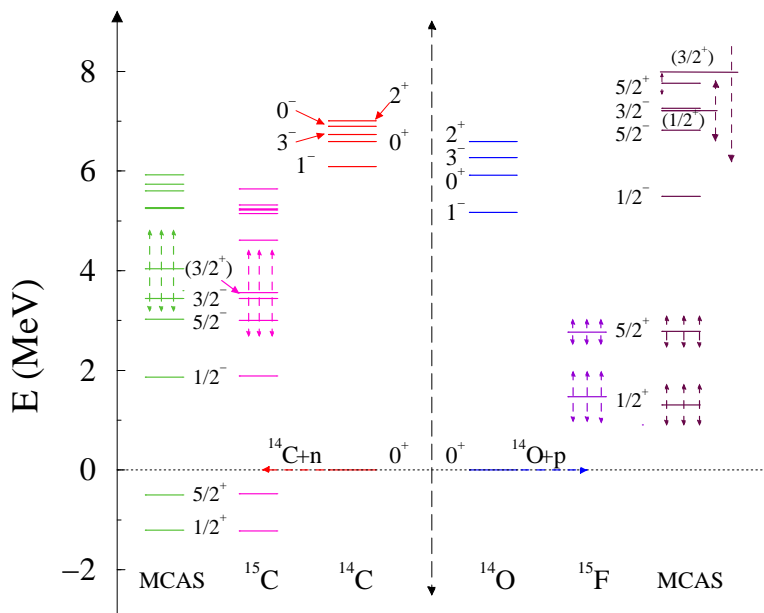


Fig. 1. Low energy spectra of $^{14,15}\text{C}$ and of $^{14,15}\text{O}$, empirical⁴ and from results of MCAS calculations. The zero of energy is set to that of the relevant mass-14 ground state.

Details have been specified fully in a recent paper.³ The spectrum of ^{15}C has two bound states of spin-parities $\frac{1}{2}^+$ (ground) and $\frac{5}{2}^+$. They are described dominantly as a single sd shell neutron on the ^{14}C ground state. Then there are three quite narrow resonances, all having negative parity, which lie within the spread of a broad $\frac{3}{2}^+$ resonant state. That broad $\frac{3}{2}^+$ state was seen very clearly in the cross section from a measurement of $^{14}\text{C}(d,p)$. It is noteworthy that there are no other bound states; in particular none having negative parity. Such would occur if, in the $n+^{14}\text{C}$ system, the $0p_{\frac{1}{2}}$ neutron orbit was not Pauli blocked. However, there are negative parity resonances, and to find them in our evaluations of ^{15}C , required that the neutron $0p_{\frac{1}{2}}$ orbit only be Pauli hindered.³ With the nuclear interaction set, by including Coulomb interactions in MCAS evaluations, properties of the $p+^{14}\text{O}$ system (giving particle unstable ^{15}F) were determined. Those results are shown on the right of Fig. 1.

The two lowest resonance states of ^{15}F have been observed in scattering cross-sections. Those data,^{5,6} and our results, are shown in Fig. 2. In the top panel we show the cross sections from ^{14}O scattering from hydrogen. The MCAS result (solid

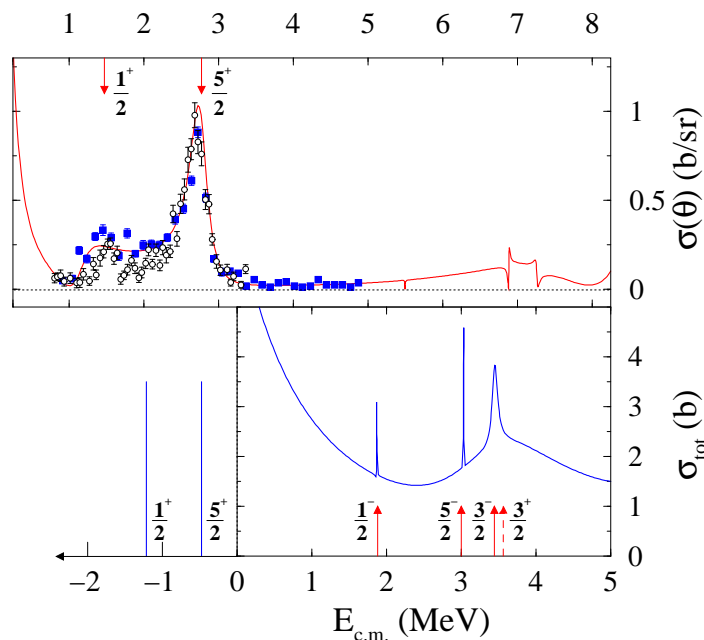


Fig. 2. The elastic cross sections from scattering of ^{14}O ions from hydrogen at $\theta_{c.m.} = 180^\circ$ (top) and the predicted (MCAS) total cross section for $n\text{-}^{14}\text{C}$ scattering (bottom).

curve) compares reasonably well with the data and it is as good as has been found with other analyses.³ In the bottom panel of Fig. 2 is a prediction of the total scattering cross section of neutrons from ^{14}C for energies to 5 MeV. There are four obvious resonances; three quite narrow (of negative parity) and a very broad $\frac{3}{2}^+$ one. The three narrow resonances have partners in the $p\text{-}^{14}\text{O}$ cross section. That is shown in the top panel, while the broad $\frac{3}{2}^+$ structure becomes more complex and overlaps with two other states. The zero of the energy scale has been placed to optimally match the $\frac{5}{2}^+$ bound state in ^{14}C to the centroid of the analogous resonance state in ^{15}F .

Analogues of the negative parity resonances in ^{15}C are predicted in ^{15}F . But the origin of these new, narrow negative-parity resonances in ^{15}F differ from those of the observed low-lying ones. They are compound resonances and are very affected by the Pauli-hindrance of the proton $0p_{\frac{1}{2}}$ orbit in the $0_{\frac{1}{2}}^+$ and 2^+ excited states of ^{14}O .

3.2. Spectra of ^7He , ^7Li , ^7Be , ^7B

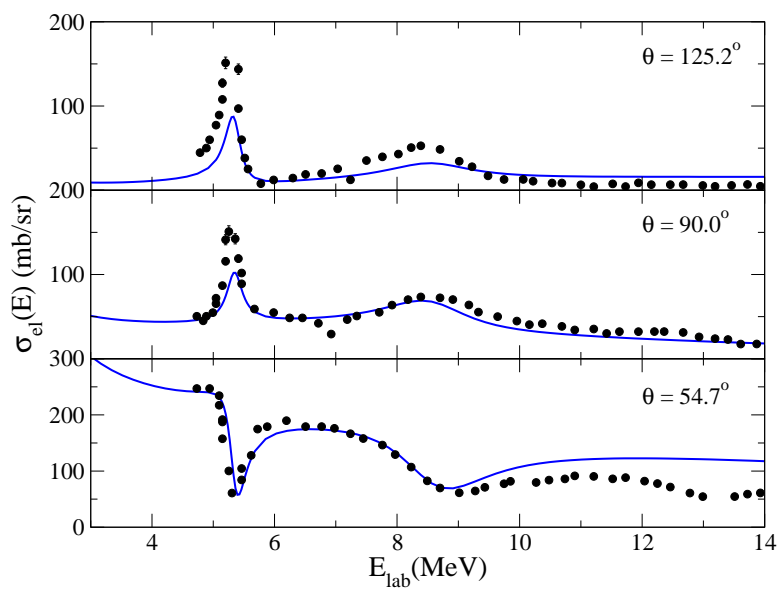
A single nuclear interaction matrix of potentials was found whose use with appropriate Coulomb terms in MCAS calculations gave spectra of these nuclei in good agreement with known ones. For ^7Li ($p\text{-}^6\text{He}$) and ^7Be ($n\text{-}^6\text{Be}$), the results are listed in Table 1. Therein the numbers in square brackets are the known experimen-

Table 1. Bound spectra of ${}^7\text{Li}$ and of ${}^7\text{Be}$ ^a.

| J^π | ${}^7\text{Li}$ Exp. | $p+{}^6\text{He}$ | ${}^3\text{H}+{}^4\text{He}$ | ${}^7\text{Be}$ Exp. | $n+{}^6\text{Be}$ | ${}^3\text{He}+{}^4\text{He}$ |
|------------------|----------------------|-------------------|------------------------------|----------------------|-------------------|-------------------------------|
| $2\frac{1}{2}^-$ | -10.0 | -10.0 | -10.3 | -10.7 | -11.0 | -10.1 |
| $1\frac{1}{2}^-$ | -9.5 | -9.5 | -9.74 | -10.2 | -10.7 | -9.88 |
| 1^- | -5.3 [0.06] | -5.3 | -5.4 [0.08] | -6.1 [0.18] | -6.4 | -6.0 [0.18] |
| $3\frac{1}{2}^-$ | -3.4 [0.92] | -3.4 | -3.3 [0.83] | -4.0 [1.2] | -4.5 | -4.0 [1.19] |
| 2^- | -2.3 [0.08] | -0.3 | | -3.5 [0.44] | -1.6 | |
| 1^- | -1.2 [4.7] | -2.2 | | -- | -- | |
| 3^- | -0.9 [2.8] | -0.9 | | | -2.1 | |
| $2\frac{1}{2}^-$ | -0.4 [0.44] | -0.4 | | -1.4 [?] | -1.7 | |
| $1\frac{1}{2}^-$ | -- | -- | | -0.8 [1.8] | -3.3 | |

Note: ^a All energies are in reference to nucleon + mass 6 nucleus thresholds

tal widths obtained from $t+\alpha$ (${}^3\text{He}+\alpha$) reactions. The nucleon emission thresholds lie higher and so no nucleon widths arise from the MCAS calculations. However, those evaluations produced 12 states to 15 MeV excitation in ${}^7\text{Li}$ with the lowest 9 matching known spin-parity states in the spectrum. The next three calculated levels are in the energy region in which two resonant states of undetermined spin-parity are known. The five lowest lying states in the known spectrum of ${}^7\text{Be}$ compare reasonably with the MCAS values. The calculations give more states than are known to date above an excitation energy of ~ 8.5 MeV, and there are a few crossings.

Fig. 3. Cross sections from $\alpha({}^3\text{He},{}^3\text{He})\alpha$ scattering.

To consider other open reaction channels, we have used MCAS to evaluate ${}^3\text{H}$ - and ${}^3\text{He}$ - α scattering using a potential model form of a cluster system. A nuclear interaction was found that gave the results listed in the fourth and seventh columns in Table 1. The calculated results agree well with the known values. Note that the energies are listed relative to the relevant nucleon+nucleus thresholds.

We used that interaction with MCAS to find elastic scattering cross sections at three center of mass scattering angles ($54.7^\circ, 90.0^\circ, 125.2^\circ$) at which data have been taken. The results of some of those calculations are shown by the solid curves in Fig. 3. The comparisons with data are very good, adding confirmation to our definition of the basic di-cluster-interaction potential.

3.3. MCAS and capture cross sections

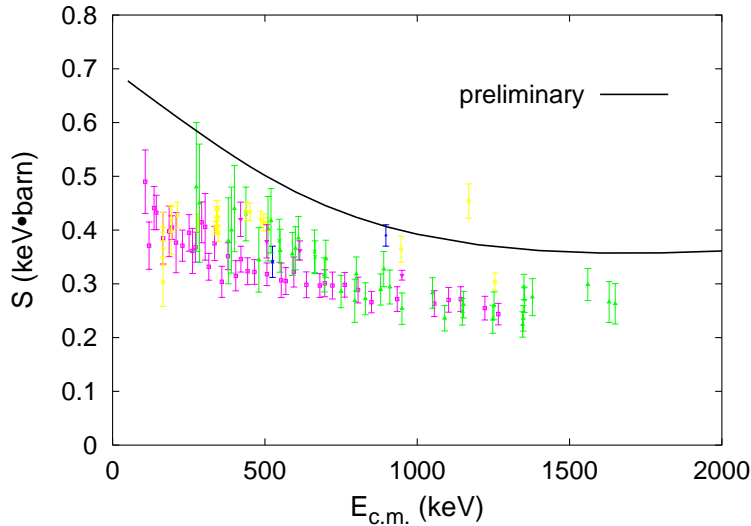


Fig. 4. The calculated astrophysical S -factor from ${}^3\text{He}$ - ${}^4\text{He}$ capture compared with data.⁷

Recently, Canton, Levchuck, and Shebeko⁸ used the MCAS di-cluster model wave function, though with an approximate scattering wave function (hence the results are preliminary), to evaluate the radiative capture cross section $\sigma_R(E)$ and from which the astrophysical S -factor is determined by

$$S(E) = \sigma_R(E) E \exp \{2\pi\eta(E)\}. \quad (7)$$

Therein $\eta(E)$ is the Sommerfeld parameter. The results of the calculated S -factor are compared in Fig. 4 with data.⁷ The calculated S -factor overestimates the measured data but by only 20%. There has been no arbitrary scaling used, i.e. no asymptotic normalization or adjusted spectroscopic factor. Given that the bound state of ${}^7\text{Be}$

is not expected to be 100% a di-cluster, these results are most encouraging. Of note, both scattering and bound state functions can be given by MCAS so that there is no orthogonality problem as in past radiative capture calculations.

4. Conclusions

Applications of the MCAS theory have been made to discern the structure of the compound nuclei underlying various di-cluster nuclear systems of light mass. Despite the simplicity of the collective model potentials used, good agreement has been found with available data, even regarding a nucleus lying beyond the proton drip line. Use of MCAS information to evaluate radiative capture cross sections is a promising new development.

5. Acknowledgements

This research was supported by the Italian MIUR-PRIN Project “Fisica Teorica del Nucleo e dei Sistemi a Più Corpi”, by the Natural Sciences and Engineering Research Council (NSERC), Canada, and by the National Research Foundation of South Africa.

References

1. K. Amos, L. Canton, G. Pisent, J. P. Svenne and D. van der Knijff, *Nucl. Phys.* **A728**, p. 65 (2003).
2. L. Canton, G. Pisent, K. Amos, S. Karataglidis, J. P. Svenne and D. van der Knijff, *Phys. Rev. C* **74**, p. 064605 (2006).
3. L. Canton, G. Pisent, J. P. Svenne, K. Amos and S. Karataglidis, *Phys. Rev. Lett.* **96**, p. 072502 (2006).
4. F. Ajzenberg-Selove, *Nucl. Phys.* **A523**, p. 1 (1991).
5. V. Z. Goldberg *et al.*, *Phys. Rev. C* **69**, p. 031302(R) (2004).
6. F. Q. Guo *et al.*, *Phys. Rev. C* **72**, p. 034312 (2005).
7. D. Bemmerer *et al.*, *Phys. Rev. Lett.* **97**, p. 122502 (2006).
8. L. Canton, L. Levchuck and A. Shebeko, (2007), (private communication).